Beveled Osteotomies in Lateral Orbitotomy Using a Customized Rotating Bone Saw for Orbital Neoplasms

Maria Donna Damo Santiago, MD, MBA[1,2] Prospero Maria Tuano, MD[3]

[1] Department of Ophthalmology, Far Eastern University-Nicanor Reyes Memorial Foundation (FEU-NRMF), Quezon City, Philippines
[2] Department of Ophthalmology, St. Luke's Medical Center, Quezon City, Philippines
[3] Department of Ophthalmology, University of the Philippines, Philippine General Hospital, Manila, Philippines

Address for correspondence Maria Donna Damo Santiago, MD, MBA, Department of Ophthalmology, Far Eastern University-Nicanor Reyes Memorial Foundation (FEU-NRMF), Regalado Avenue, North Fairview, Quezon City, Philippines 1123 (e-mail: donsantmd@yahoo.com; donsantiagomd@yahoo.com.ph).

Craniomaxillofac Trauma Reconstruction 2015;8:141–149

Abstract

This study aims to develop a novel method of beveled osteotomy for lateral orbitotomy using a customized 21-mm stainless steel rotating saw in lateral orbitotomy and to evaluate the outcome of a novel beveled osteotomy in lateral orbitotomy. This article presents a case series (19 orbits from 18 patients) of lateral orbitotomies for excision biopsy of orbital neoplasms, over a 10-year period (from September 2001 to October 2011). It is a retrospective observational study. The surgeries were performed under the primary service of one surgeon (M. D. D. S.), the author of this study. All patients were treated via beveled osteotomies in lateral orbitotomy using a stainless steel, 21 mm diameter, customized rotating bone saw. Preoperative and postoperative measurements were tabulated and statistically analyzed. The case series demonstrated that beveled osteotomies in lateral orbitotomy using a stainless steel, 21 mm diameter, customized rotating bone saw was technically possible and provided access to lateral subperiorbital, peripheral, and central surgical spaces. The exposure was ample for excision biopsy of all neoplasms in this study. No patient needed the use of miniplate hardware in repositioning the lateral orbital wall nor complained of a palpable deformity of the lateral orbital wall. The wound healing was rapid, with minimal tissue distortion or scars. There were two patients who developed skin burns, but neither required a cosmetic surgery to correct scarring from the burn. It was concluded that the modified technique of beveled osteotomies in lateral orbitotomy provides excellent access to the lateral subperiorbital, peripheral and central surgical spaces. The exposure was adequate for excision biopsy of all neoplasms in this study. The technique promotes osseous union without the use of miniplate hardware. The use of a stainless steel 21 mm diameter customized rotating bone saw facilitated the successful outcome of the beveled technique.

Keywords
- osteotomies
- orbitotomies
- beveled
- neoplasms

Orbital procedures can be difficult, even to the experienced orbital surgeon. Recent advances in imaging modalities, surgical techniques, and instrumentation have transformed and modernized our approach in the management of orbital lesions. The surgical technique used depends on the location of the lesion and the level of comfort of the surgeon. The

received
July 2, 2013
accepted after revision
February 12, 2014
published online
November 12, 2014

DOI http://dx.doi.org/10.1055/s-0034-1393723.
ISSN 1943-3875.

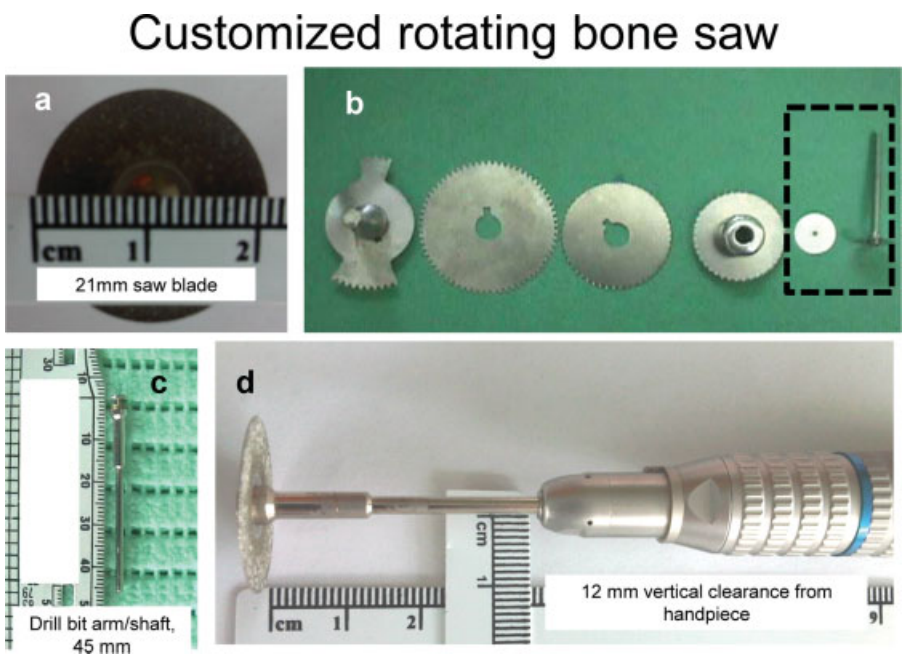

Fig. 1 (**a, b**) Customized rotating saw blade measuring 21 mm in diameter, 0.3 mm in thickness. (**c**) A 45-mm drill bit shaft. (**d**) Vertical clearance of 12 mm from surface to the drill handle.

lateral approach allows the best exposure to the lacrimal gland fossa and the posterior orbit including the intraconal space. Kronlein original technique, which was described in the late 1800s, has been modified on numerous occasions, by Berke, Reese, Wright, and others.[1–4]

Complications can occur following orbital surgery. These include orbital hematomas, motility disturbance, pupillary abnormalities, eyelid malpositions, and cerebral spinal fluid leakage.[5] Complications relating to the creation of a bone flap, include non/malunion of the bones, which can result in cosmetic deformity and the need for miniplate hardware in bone repositioning.

Although traditional blunt-force osteotomy techniques remain an indispensable tool in bone surgery,[6] power-assisted instrumentation offers a useful alternative for controlled bone resection. It facilitates precise bone removal and three-dimensional sculpting without the soft tissue trauma characteristic of manual osteotomy.

It is desirable to use the most modern instruments available; however, cost efficiency is one of the primary considerations in the surgical management of patients in a developing country such as the Philippines. Oscillating saws were not available in the hospitals where the lateral orbitotomies in the study were done.

The stainless steel, customized rotating bone saw, used in the current study costs only about $10 per piece. Even if one adds to this amount, the cost of an ordinary micromotor dental drill, which can be sourced for less than $100, the total cost would still be less expensive than that of an oscillating bone saw.

This article does not specifically address indications or benchmark outcomes for lateral orbitotomy but instead proposes a novel modification of the well-accepted surgery, one that promotes the creation of beveled osteotomies using a customized rotating bone saw.

Methods

A retrospective review of records for all the patients who underwent "beveled osteotomies in lateral orbitotomy using a 21-mm diameter customized rotating bone saw" from September 2001 to October 2011was performed.

The basic elements of the mechanism for the beveled osteotomy construction include the 21-mm stainless steel customized saw (►**Fig. 1a, b**) rigidly affixed to the 45-mm drill bit shaft (►**Fig. 1c**) inserted into the guide slot of a straight nosecone handpiece (Nakanishi NSK, Tochigi, Japan) and the drive gear rotated by a commonly available electric surgical power head (dental micromotor, Sunburst, China). The mechanism produces the desired rotational motion of the circular saw blade about its axis at a speed of up to 35,000 rpm. The saw blade is placed at the top of the intended cuts in the bone, moving the blade in a beveled orientation, down into the bone as the cut proceeds. There is a 12-mm vertical clearance from the surface to the drill handle (►**Fig. 1d**).

Our novel technique of beveled osteotomy for lateral orbitotomy is ensured by the application of the circular bone saw obliquely to the surface of the bone at the osteotomy sites. An oblique bone cut allows separated bones to be lengthened with increased point of contact (►**Fig. 2a**), while a transverse plane cut through the bone will produce flat opposing surfaces (►**Fig. 2b**). The horizontal lines drawn across the lateral rim show the starting point of the superior osteotomy at the anterior lateral orbital rim to be at least 2 mm lower than its posterior extent, while the starting point

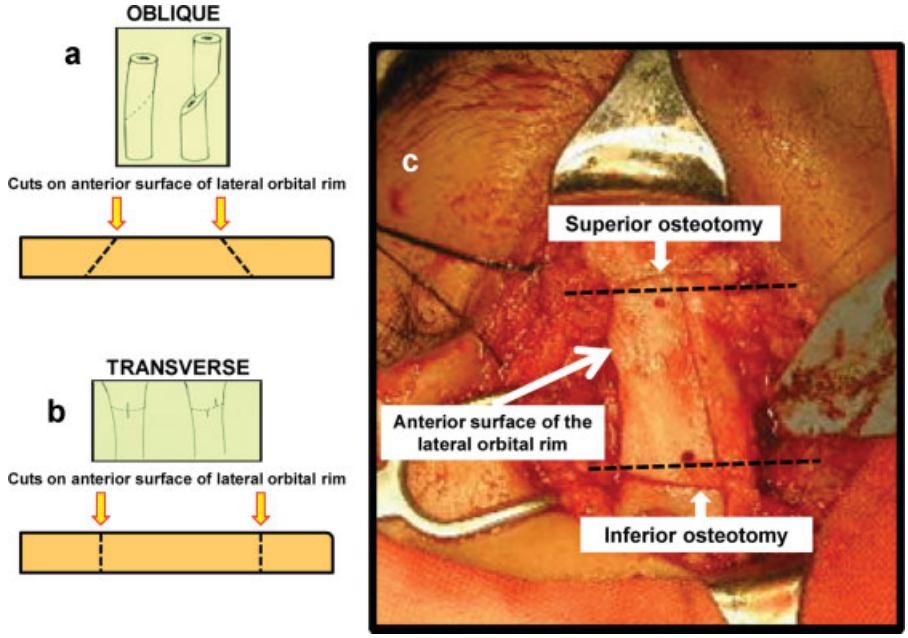

Fig. 2 (**a**) Oblique osteotomy. (**b**) Transverse osteotomy. (**c**) Intraoperative photo demonstrating beveled osteotomies superiorly and inferiorly for lateral wall removal and en bloc removal of the deep lateral wall.

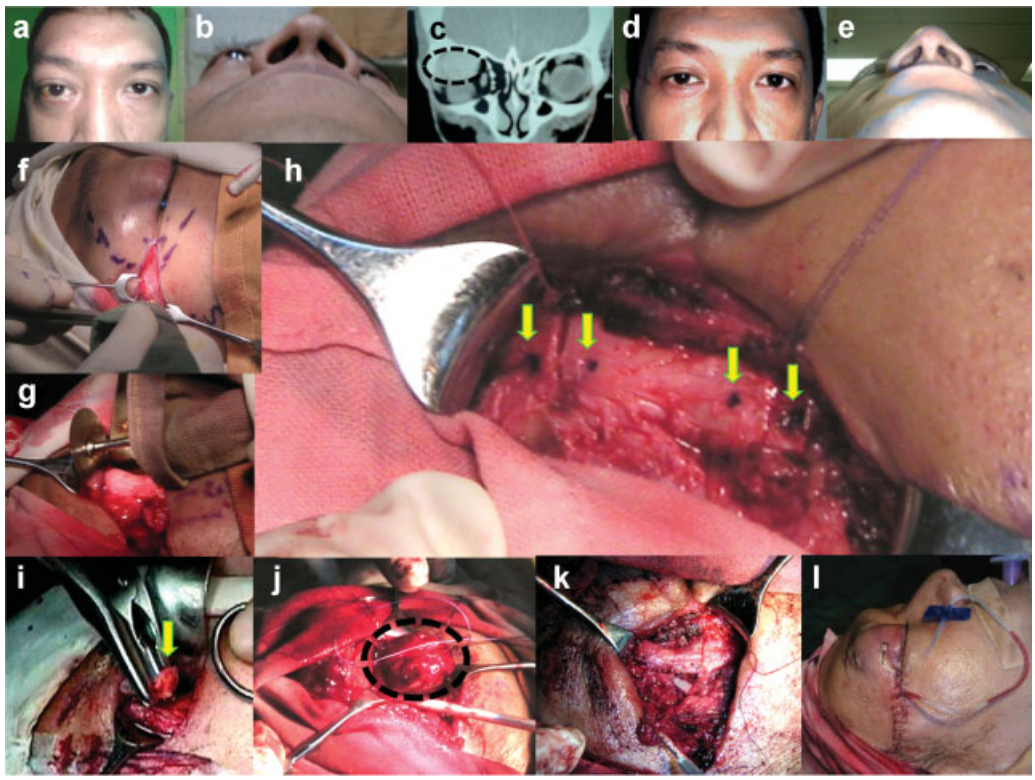

Fig. 3 (**a, b**) Preoperative photographs of case no. 15, demonstrating proptosis of the right side. (**c**) Coronal CT scan showing a well-delineated mass (cavernous hemangioma, encircled) at the superotemporal aspect of the right orbit. (**d, e**) Postoperative photographs after 4 months showing the resolution of proptosis. (**f**) A 1.5-cm tendon-sparing, lateral canthal incision. (**g**) Beveled osteotomy through the lateral orbital rim using the 21-mm customized rotating bone saw, (**h**) 1-mm burr holes (arrows) drilled superior and inferior to each planned osteotomy for refixation with suture if required. (**i**) Removal of the lateral rim (arrow) via an en bloc osteotomy. (**j**) The orbital mass (encircled) excised. (**k**) The lateral orbital rim returned to its original position. (**l**) Placement of a fenestrated butterfly drain before closure. CT, computed tomography.

of the inferior osteotomy is 2 mm or higher than its posterior extent (►**Fig. 2c**). The technique effectively produces a wider posterior opening that would maximize surface area contact for the repositioned bone flap after excision of the neoplasm. This beveled technique also allows osteotomies to be stabilized without fixation. The use of the customized rotating saw facilitated the creation of the beveled osteotomies through its precise cuts that produced a minimal bone loss.

Visual acuity, Hertel exophthalmometry measurements, optic nerve changes, for example, disc edema, optic disc pallor, and the presence of diplopia, were evaluated in all patients preoperatively and postoperatively. Preoperative imaging via computed tomography (CT), magnetic resonance imaging (MRI) or both were done. Proper informed consent enumerating the possible risks and complications of surgery were secured from all patients before surgery. Informed consent for the use of photographs relating to the case, for medical, scientific or educational purposes, were likewise secured. Preoperative oral antibiotics and combined antibiotic–steroid ophthalmic solution were administered. After induction of general endotracheal anesthesia, the periorbital region was anesthetized with subcutaneous injection of 2% lidocaine with epinephrine.

Pupil size and light reflex were noted preoperatively. The cornea was protected with a corneal protector coated with ophthalmic ointment. A 1.5-cm lateral canthal incision beginning 10 mm from the lateral canthal angle to spare the lateral canthal tendon, was then made with a no. 15 blade and dissection proceeded to the lateral orbital rim (►**Fig. 3f**). The periosteum was incised with the Ellman microneedle (Ellman International, Hewlett, NY) in cutting coagulation waveform, and was dissected off of the lateral orbital wall both laterally and medially, using malleable retractors for exposure. The temporalis muscle was retracted as necessary and was not detached. Meticulous hemostasis was maintained. The inferior extent of the osteotomy was marked adjacent to the floor of the orbit above the zygomatic arch. The maximal superior extent of the osteotomy was marked at 5 mm above the frontozygomatic suture. Using appropriate orbital protection with malleable retractors, beveled osteotomies were made superiorly and inferiorly through the lateral orbital rim using a customized rotating bone saw (►**Fig. 3g**). One millimeter holes were drilled superior and inferior to each planned osteotomy (►**Fig. 3h**) for refixation with sutures should further stabilization be desired. Copious irrigation with normal saline solution was done during the osteotomy. The lateral orbital bone was removed via an en bloc osteotomy (►**Fig. 3i**). The orbital mass was exposed, dissected free from surrounding orbital tissues, excised and sent for histopathology (►**Fig. 3j**). The lateral orbital rim was returned to its original position (►**Fig. 3k**). Fixation at burr holes with Prolene 4–0 sutures was optional. The deep layers of fascia were closed with 5–0 Vicryl (Ethicon Surgical, Somerville, NJ) sutures and skin closure was accomplished with 6–0 Prolene sutures (Ethicon Surgical). Before closure, a fenestrated butterfly drain (►**Fig. 3l**) was placed in the orbit and sutured to the skin with 6–0 Silk (Ethicon Surgical).

Results

In total, 19 orbits of the 18 patients underwent this technique. The patients' average age was 34 years. Seven patients were males and 12 females. The average follow-up interval was 20 months (range, 2–74 months). The most common presenting sign was proptosis (47%) followed by diplopia (21%) and blurred vision (11%). Eight (42%) of the 19 orbits involved the right side ►**Table 1**.

Preoperative imaging was done in all cases: CT in 16 (84%) cases, MRI in 2 (11%) cases, and both CT and MRI in 1 (5%) case. The biggest volume documented through imaging was for a lacrimal gland pleomorphic adenoma in case no. 8, and smallest for an epidermoid cyst in case no. 10 ►**Table 2**.

Visual acuity was measured in all cases preoperatively and postoperatively (►**Fig. 3**). The postoperative visual acuity was the same as the preoperative visual acuity in 12 (63%) cases. Four (21%) cases recorded improved visual acuity with an average gain of two lines. Three (16%) cases showed decreased postoperative visual acuity. Among those who recorded a decrease in Snellen acuity was case no. 5, who sustained skin burns proximal to the incision postoperatively,

Table 1 General information of 19 consecutive cases of beveled osteotomies in lateral orbitotomy using a customized rotating bone saw for orbital neoplasms

	Value, *n* (%) (± SD) [Range]
Gender	
Male	7 (37)
Female	12 (63)
Age (y)	34.63 (± 16.58) [8–75]
Affected eye	
Right	8 (42)
Left	11 (58)
Presenting sign	
Proptosis	9 (47)
Reduced visual acuity	2 (11)
Diplopia	4 (21)
Mass	1 (5)
Inflammatory (redness, swelling)	1 (5)
Headache	1 (5)
Hyperlacrimation	1 (5)
Preoperative visual acuity (decimal acuity, best corrected, involved eye)	0.68 [20/20–NLP[a]]
Follow-up (mo)	
Mean	20.36 (± 21.56) [2–74]
Median	14

[a]Preoperative visual range in Snellen acuity.

Table 2 Imaging, lesion size, duration of surgery, postoperative gain in Snellen acuity, exophthalmometry improvement, and histopathological diagnosis of 19 cases of beveled osteotomies in lateral orbitotomy using a customized rotating bone saw for orbital neoplasms

Patient	Imaging	Lesion size (mm)	Duration of surgery (h)	Postoperative gain in visual acuity (Snellen lines)	Exophthalmonmetry improvement (mm)	Histopathologic diagnosis
1	CT	25 × 18 × 10	3.75	0	5	Cavernous hemangioma
2	CT	32 × 29 × 14	3.86	3	4	Pleomorphic adenoma, lacrimal gland
3	CT	28 × 20 × 15	3.62	0	0	Adenocarcinoma, lacrimal gland
4	CT	20 × 25 × 29	3.71	0	2	Cholesterol granuloma
5	CT	24 × 22 × 18	2.80	−1	3	Epithelial inclusion cyst
6	CT	13 × 23 × 12	3.58	0	2	Cavernous hemangioma
7	CT and MRI	12 × 24 × 14	2.83	0	3	Schwannoma
8	CT	38 × 32 × 15	3.77	1	6	Pleomorphic adenoma, lacrimal gland
9	CT	21 × 27 × 32	3.53	3	6	Dermoid
10	CT	16 × 14 × 12	2.66	3	1	Epidermoid cyst
11	CT	26 × 21 × 17	3.33	0	2	Cavernous hemangioma
12	CT	17 × 19 × 20	4.16	−3	5	Meningioma
13	CT	20 × 20 × 11	3.23	−2	4	Schwannoma
14	CT	45 × 30 × 12	4.80	0	5	Cholesterol granuloma
15	CT	24 × 23 × 12	4.17	0	6	Cavernous hemangioma
16	MRI	33 × 14 × 25	7.58	0	4	Cavernous hemangioma, recurrent
17	MRI	25 × 25 × 15	3.87	0	3	Adenocarcinoma, lacrimal gland
18	CT	32 × 20 × 10	4.58	0	3	Pleomorphic lipoma
19	CT	28 × 25 × 10	4.16	0	2	Dacryoadenitis

Abbreviations: CT, computed tomography; MRI, magnetic resonance imaging.

(►**Fig. 4**). Postoperative examination revealed central serous retinopathy in the operated eye. The patient was then referred to a vitreoretinal specialist and her post–laser treatment vision in the affected eye was 20/25, one line less than her preoperative visual acuity. The other patients with decreased vision were case no. 12 with meningioma and case no. 13 with schwannoma. Case no. 12 was a 29-year-old female patient with meningioma of the left side (►**Fig. 5**). CT scans showed a spindle-shaped lesion along the intraconal portion of the left optic nerve extending into the intracranial segment up to the chiasm (►**Fig. 5b, c**). The circumferential nature of the lesion caused optic nerve compression and optic disc edema of the left eye (►**Fig. 5e**). Best corrected visual acuity in the affected eye was only 20/70 compared with the fellow eye with visual acuity of 20/20. The patient and her family were informed regarding the consequent visual loss with excision biopsy of the mass due to its location, but they insisted on the surgical option despite assurances that the mass is most probably benign. Case no. 13 was a 75-year-old female patient, with schwannoma and chronic bilateral nasolacrimal duct obstruction that caused epiphora. The persistent tearing was identified as the cause of decreased visual acuity postoperatively.

Hertel exophthalmometry measurements improved in 18 (95%) cases. The average exophthalmometry improvement was 3.5 mm (SD ± 1.74) (range, 1–16 mm). The only patient who did not demonstrate any improvement in proptosis was a 19-year old case no. 3 with adenocarcinoma of the lacrimal gland. The patient subsequently underwent exenteration in another institution. There was postoperative resolution of diplopia in three out of the four cases.

The duration of surgery with the technique of beveled osteotomies in lateral orbitotomy using a customized rotating bone saw averaged almost 4 hours (mean 3.96 hours; median 3.75 hours; SD ± 1.08). It was shortest at 2.66 hours for case no. 10 of an epidermoid cyst on a 54-year-old female patient.

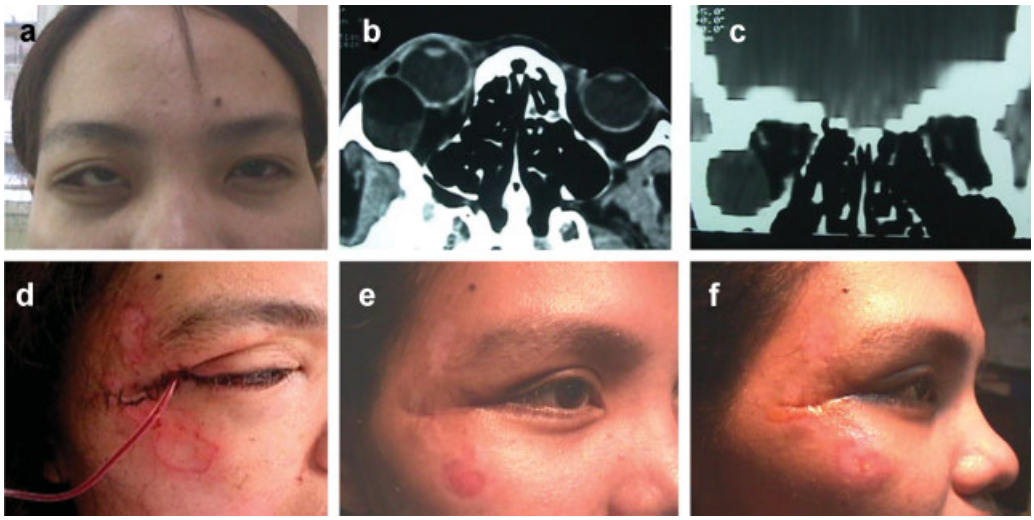

Fig. 4 (**a**) Preoperative photograph of case no. 5 showing the medial displacement of the right globe. (**b**) Axial and, (**c**) reformatted coronal CT documenting a mass on lateral aspect of the right orbit. (**d**) Skin burns proximal to the incision site at postoperative day 1. (**e**) Skin burns at 3 weeks postoperatively. (**f**) Skin burns at 6 weeks postoperatively. CT, computed tomography.

The longest duration of surgery about 7.58 hours was in case no. 16 of a recurrent cavernous hemangioma in a 32-year-old female patient, who previously underwent excision biopsy through lateral orbitotomy with bone flap in two other institutions. No significant lesion size–duration of surgery relationship was observed in our patient series. There was only a weak positive correlation ($r = 0.22, p = 0.01$) between the size of the orbital neoplasm determined by preoperative CT/MRI imaging and the duration of surgery.

Only five patients underwent postoperative CT, due to financial constraints. All five patients demonstrated evidence of osseous union, with the earliest documented at 3 months postoperatively. In case no. 9, previously operated for dermoid cyst, CT evidence of osseous union was noted by direct visualization on resurgery via the same technique (►**Fig. 6**). There was no increased difficulty in utilizing the same superior and inferior osteotomies for the repeat procedure.

Two patients, case no. 5 (►**Fig. 4**) and case no. 7, sustained skin burns from overheating of the electric powered rotary surgical handpiece. During the surgical osteotomy, the rotary handpiece driving the bone saw overheated and burned soft tissues near the incision. None of these patients required cosmetic surgery to correct scarring from the burn.

In case no. 1, the lateral orbitotomy was combined with an anterior approach to obtain better access to the superomedially located cavernous hemangioma in an orbit with a 20/30 best corrected vision. The patient required ptosis surgery postoperatively (►**Fig. 7**).

No patient in the study required the refixation of the lateral wall with nonabsorbable sutures through the

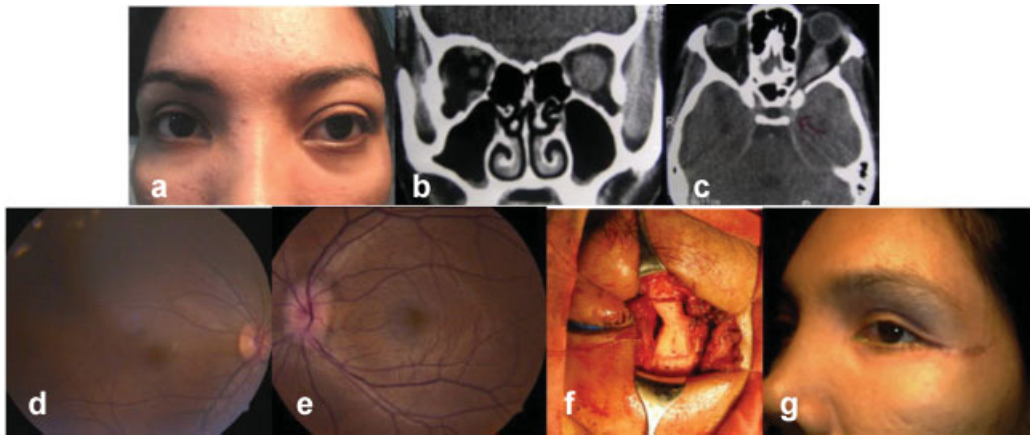

Fig. 5 (**a**) Preoperative photograph of case no. 12, demonstrating axial proptosis of the left side. (**b, c**) Coronal and axial CT scans showing an inhomogenously enhancing spindle-shaped lesion along the intraconal portion of the left optic nerve extending into the intracranial segment up to the chiasm. (**d, e**) Optic disc photographs of the right and left eye documenting the disc edema on the affected eye. (**f**) Beveled osteotomies through the lateral orbital rim using the 21-mm customized rotating bone saw. (**g**) Postoperative photograph after 6 months showing the resolution of proptosis and incision scar. CT, computed tomography.

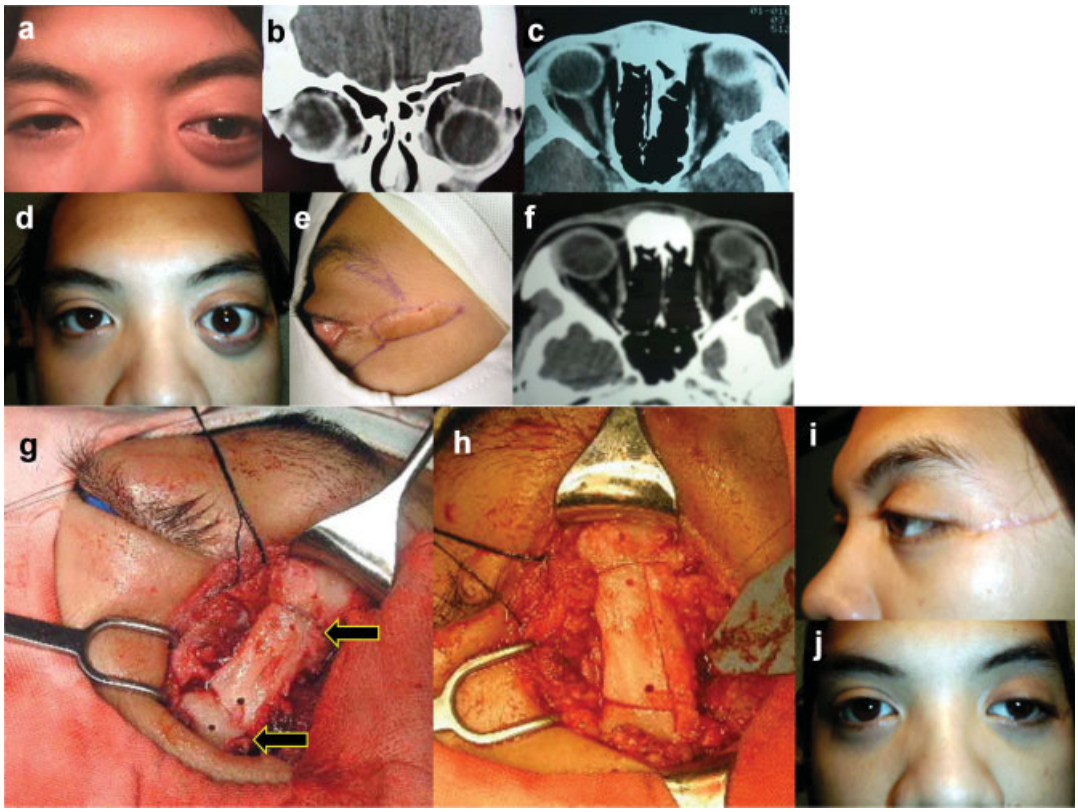

Fig. 6 (**a**) Preoperative photograph of case no. 9 showing proptosis of the left side. (**b**) Coronal and (**c**) axial CT scans documenting a well-delineated mass (dermoid) at the superotemporal aspect of the left orbit. (**d**) Photograph on follow-up 6 years postoperatively with recurrence of proptosis and, (**e**) scar at the incision site. (**f**) Repeat axial CT scan documenting the osseous union at previous osteotomy sites and the presence of an orbital mass. (**g**) Osseous union of superior and inferior osteotomies (arrows) visualized at the time of surgery; these same sites were used for the repeat procedure. (**h**) The lateral orbital rim returned to its original position after excision of cholesterol granuloma. (**i, j**) Photographs 2 months postoperatively with scar revision. CT, computed tomography.

preosteotomy burr holes, nor stabilization with the use of miniplate hardware. There were no unstable malunion of the lateral orbital bones. No patient complained of painful, palpable, or cosmetically objectionable facial deformity due to the procedure.

Discussion

This study presents a modified technique for performing osteotomies in lateral orbitotomy with bone flap for orbital neoplasms. The approach utilized differs from the conventional technique in that the cuts through the lateral orbital wall were beveled and done using a stainless steel, 21 mm diameter, and customized rotating bone saw.

The beveled incision can be performed with the customized rotating bone saw or the commercially available oscillating saws. In the authors' opinion, the beveled osteotomies in lateral orbitotomy would be of benefit for either modality. Gilliland and Clayton used a lateral wall advancement technique through beveled superior and inferior osteotomies in their modified graded-balanced orbital decompression for patients with severe thyroid orbitopathy. There was a harvest of the cortical bone of the greater wing of the sphenoid via an en bloc osteotomy, which was used as the interpositional bone graft. They also utilized an image-guided surgical navigation equipment, intraoperatively. The bone grafts harvested en bloc were cut to shape and fixated with screws.

Our technique in this study is similar to Gilliland and Clayton with respect to the beveled cuts for lateral wall removal and en bloc removal of the deep lateral wall. Unlike their technique, no intraoperative image-guided surgical navigation equipment was employed, nor bone graft interpositioning with plates and osteoplasty with Mimix (Walter Lorenz Surgical, Jacksonville, FL). Also, the Gilliland and Clayton technique prevented the hollowing of the temporal fossa through reattachment of the temporalis muscle to the advanced lateral orbital rim with 4–0 nylon sutures through two drill holes in the posterolateral aspect of the advanced lateral rim. The authors concluded that the surgical technique provides good aesthetic results with minimal palpable deformities and promotes osseous union by maintaining "bone on bone" contact through the healing phase.[7–9] In the present study, where a similar technique of beveled osteotomies was applied, the temporalis muscle was not detached and osseous union was confirmed by both postoperative CT imaging and direct observation.

Powell et al used longitudinal in vivo micro-CT imaging to monitor bone resorption in a rat fibula osteotomy model. Quantitative image postprocessing techniques were developed for spatially aligning the longitudinal datasets to exhibit

Fig. 7 (**a**) Preoperative photograph of case no. 1 with proptosis of the left orbit. (**b**) Axial and (**c**) coronal CT scans showing a well-delineated mass at the superomedial aspect of the left orbit, (**d**) intraoperative photograph of beveled osteotomy in lateral orbitotomy. (**e**) Excision biopsy of orbital mass (cavernous hemangioma). (**f**) Wound closure showing anteromedial extension of the incision. (**g**) Postoperative ptosis of the left upper eyelid. (**h**) Ptosis surgery via frontalis suspension. (**i**) Photograph after 2 months of post–ptosis surgery.

detectable changes in bone structure over time.[10] This method could be potentially useful in the validation of observed surface area contact for the repositioned bone flap, created in a beveled fashion using the customized bone saw.

Our novel method of beveled osteotomy did not result in any incident of unstable malunion of the lateral orbital bones. This is in contrast to the published study of Borrelli et al, where straight osteotomies resulted in osseous nonunion, necessitating placement of miniplates for stability.[9] Furthermore, miniplate hardwares are frequently palpable and associated with postoperative morbidity. No patient in the present study required the use of miniplate hardware. The most common complication noted with our beveled osteotomy technique was patient burns from the rotary surgical handpiece. Two patients sustained skin burns from overheating of the electric powered rotary surgical handpiece during the surgical osteotomy. Both cases were done during the early part of this study in 2002. Rotary surgical handpieces have some form of bearings that permit the cutting tools to spin at high speeds. In routine use, the bearing lubricant is slowly removed by repeated cleaning and sterilization. Poorly lubricated bearings can cause overheating of various components of surgical handpieces. In 2003, the United States Food and Drug Administration (US FDA) reported 265 injuries and malfunctions involving over heating of pneumatic and electric powered rotary surgical handpieces. The US FDA recommended instructions to reduce the incidence of handpiece overheating, including regular servicing and lubrication.[11] In compliance with the said recommendations, the surgical handpiece was inspected and tested before every use for evidence of overheating of the bearings. Also, the manufacturer's instructions for servicing and lubrication were strictly followed. With the precautions instituted to prevent heat-related injuries, there were no subsequent incidences of burn injury associated with the use of the surgical handpiece.

Kharkar et al in his published study, which compared a nonbeveled lateral orbitotomy approach and modified hemicoronal approach in the treatment of unstable malunions of zygomatic complex fractures, reported that both groups had a temporary facial nerve injury, primarily related to retraction of the nerve.[12] None of the patients in this study manifested facial nerve injury as a postoperative complication.

The technique of performing beveled osteotomies using a 21-mm customized rotating bone saw at the superior and inferior osteotomy sites of the lateral orbital rim maximizes surface area, contact between the bones, which promotes osseous union.[13] The cosmetic deformity from a "step off" or from miniplate hardware is also eliminated.[14]

In summary, the authors propose that beveled osteotomies in lateral orbitotomy using a stainless steel, 21 mm diameter, customized rotating bone saw, is a reliable technique that provides excellent access for excision biopsy of neoplasms in the lateral subperiorbital, peripheral, and central surgical spaces. This technique decreases the risk of postoperative temporal fossa hollowing since the temporalis muscle is not detached. The stability of the reconstructed structures

supports the use of this technique as a predictable method for the reduction of proptosis and resolution of diplopia secondary to orbital neoplasms.

Statement of Ethics

We certify that all applicable institutional and governmental ethical regulations were followed during this research.

References

1 Henderson JW, Farrow GM. Orbital Tumors. 2nd ed. New York, NY: BC Decker; 1980:580–584
2 Wright JE. Surgery of the orbit. In: Miller S, ed. Operative Surgery. 3rd ed. London: Butterworth; 1976
3 Callahan A. Wright's lateral orbitotomy. In: Jakobiec FA, ed. Ocular and Adnexal Tumors. Birmingham, AL: Aesculapius Publishing; 1978:843–897
4 Wright JE, Stewart WB. Orbital surgery. Int Ophthalmol Clin 1978; 18(3):149–167
5 McCord CD, Cole HP II. Surgical Approaches to the Orbit. In: McCord CD, Tannenbaum M, eds. Oculoplastic Surgery. 3rd ed. New York, NY: Raven Press; 1987:477–514
6 Davis RE, Raval J. Powered instrumentation for nasal bone reduction: advantages and indications. Arch Facial Plast Surg 2003;5(5): 384–391
7 Gilliland GD, Clayton E. Beveled osteotomy with lateral wall advancement and interpositional bone grafting for severe thyroid orbitopathy. Ophthal Plast Reconstr Surg 2007;23(3):192–196
8 Catanzariti AR. Graft-enhanced arthrodesis. J Foot Ankle Surg 1996;35(5):463–473
9 Borrelli J Jr, Prickett WD, Ricci WM. Treatment of nonunions and osseous defects with bone graft and calcium sulfate. Clin Orthop Relat Res 2003;(411):245–254
10 Powell KA, Latson L, Ibiwoye MO, et al. In vivo longitudinal assessment of bone resorption in a fibular osteotomy model using micro-computed tomography. Iowa Orthop J 2005;25:123–128
11 U.S. Food and Drug Administration. US Food and Drug Administration Patient Safety News 2003. Available at: http://www.accessdata.fda.gov/psn/. Accessed November 7, 2014
12 Kharkar VR, Rudagi BM, Halli R, Kini Y. Comparison of the modified lateral orbitotomy approach and modified hemicoronal approach in the treatment of unstable malunions of zygomatic complex fractures. Oral Surg Oral Med Oral Pathol Oral Radiol Endod 2010; 109(4):504–509
13 Pilitsis JG, Lucas DR, Rengachary SS. Bone healing and spinal fusion. Neurosurg Focus 2002;13(6):e1
14 Nesi FA, Gladstone GJ, Brazzo BG, et al. Ophthalmic and Facial Plastic Surgery. Thorofare, NJ: Slack; 2001